The causal role of α-oscillations in feature binding

Yanyu Zhang[a,b,c,d,1,2], Yifei Zhang[a,b,c,d,1], Peng Cai[a,b,c,d], Huan Luo[a,b,c], and Fang Fang[a,b,c,d,2]

[a]School of Psychological and Cognitive Sciences and Beijing Key Laboratory of Behavior and Mental Health, Peking University, 100871 Beijing, China; [b]Key Laboratory of Machine Perception, Ministry of Education, Peking University, 100871 Beijing, China; [c]Peking University-International Data Group/McGovern Institute for Brain Research, Peking University, 100871 Beijing, China; and [d]Peking-Tsinghua Center for Life Sciences, Peking University, 100871 Beijing, China

Edited by Robert Desimone, Massachusetts Institute of Technology, Cambridge, MA, and approved July 17, 2019 (received for review March 12, 2019)

The binding problem—how to integrate features into objects—poses a fundamental challenge for the brain. Neural oscillations, especially γ-oscillations, have been proposed as a potential mechanism to solve this problem. However, since γ-oscillations usually reflect local neural activity, how to implement feature binding involving a large-scale brain network remains largely unknown. Here, combining electroencephalogram (EEG) and transcranial alternating current stimulation (tACS), we employed a bistable color-motion binding stimulus to probe the role of neural oscillations in feature binding. Subjects' perception of the stimulus switched between its physical binding and its illusory (active) binding. The active binding has been shown to involve a large-scale network consisting of spatially distant brain areas. α-Oscillations presumably reflect the dynamics of such large-scale networks, especially due to volume conduction effects in EEG. We found that, relative to the physical binding, the α-power decreased during the active binding. Additionally, individual α-power was negatively correlated with the time proportion of the active binding. Subjects' perceptual switch rate between the 2 bindings was positively correlated with their individual α-frequency. Furthermore, applying tACS at individual α-frequency decreased the time proportion of the active binding. Moreover, delivering tACS at different temporal frequencies in the α-band changed subjects' perceptual switch rate through affecting the active binding process. Our findings provide converging evidence for the causal role of α-oscillations in feature binding, especially in active feature binding, thereby uncovering a function of α-oscillations in human cognition.

brain oscillations | individual α-frequency (IAF) | electroencephalogram (EEG) | transcranial alternating current stimulation (tACS) | visual feature binding

The visual world is composed of numerous features (e.g., orientation, color, and motion direction) that appear simultaneously and can be combined in many different possible ways as various objects. Different visual features are processed by segregated visual pathways and are represented by specialized brain areas (1). Therefore, how the visual system integrates these features into coherent objects and perceives the external world as a whole—referred to as the binding problem—is a fundamental challenge (2).

Two major theories have been proposed to explain how the brain solves the binding problem. Early binding theories argue that binding is based on spatiotemporal proximity of visual features and takes place at an early stage of visual processing, even in the absence of attention (3, 4). Contrastingly, later binding theories claim that feature binding occurs at a relatively late processing stage and that the parietal cortex is crucial for feature binding (5, 6). Notably, the feature integration theory (2) underscores that attention-dependent reentrant processes from the parietal cortex to the early visual cortex are critical in feature binding, which has gained support from recent studies (7–9).

Regardless of the brain areas where feature binding occurs, neural oscillations are proposed to be a possible mechanism for feature binding: Visual features belonging to the same object are coded through synchronous firing of neurons (10). Accumulating evidence shows that neural oscillations are of critical importance in communicating among brain areas (11) and integrating visual features together (12). However, the role of neural oscillations in feature binding is still unclear. Literature emphasizes that γ-band activity is responsible for feature binding (13–15). However, γ-activity usually reflects relatively localized neuronal processes (16, 17). Some kinds of feature binding require coordination by a neural network consisting of spatially separated, even distant brain areas (8, 9). α-Activity is usually recruited by such large-scale networks (18, 19). Therefore, it is natural to ask what the role of α-oscillations is in feature binding.

In this study, we used a bistable feature binding stimulus designed by Wu et al. (20) (Fig. 1). When observers fixated at the stimulus center, their perception of the color-motion binding in the effect part (right of the white dashed line in Fig. 1*A*) was bistable, switching between the physical binding and the active binding (21). Zhang et al. (9) found that the physical binding was implemented by feedforward pathways (from V2 to V4 and V5), whereas the active binding also recruited feedback pathways (from V4 and V5 to V2). The large-scale network of brain activity induced by the active binding renders this stimulus especially suitable for studying the role of α-oscillations in feature binding.

We combined electroencephalogram (EEG) and transcranial alternating current stimulation (tACS) to investigate the causal relationship between neural oscillations and feature binding. As a widely used noninvasive electrical stimulation technique, tACS allows us to target specific brain oscillations (e.g., the power and peak frequency in the α-band) and to possibly modulate perceptual and cognitive functions relying on these oscillations (22–25). We recorded subjects' EEG signals when they viewed the bistable stimulus and reported their perceptual state. Next, we examined the EEG spectrums for the 2 perceptual states (physical vs. active binding). Based on EEG findings, we applied tACS at a

Significance

Integrating visual features into a coherent scene is a challenge for the visual system known as the binding problem. Brain oscillations in the γ-band have been suggested to be a neural substrate of feature binding. Using electroencephalogram, we showed that feature binding was closely associated with α-oscillations. Through the entrainment of α-oscillations by transcranial alternating current stimulation, selectively changing α-oscillations could shape feature binding. Our study demonstrates the causal role of α-oscillations in feature binding and reveals a function of α-oscillations in human cognition.

Author contributions: Yanyu Zhang, P.C., H.L., and F.F. designed research; Yanyu Zhang, Yifei Zhang, P.C., and F.F. performed research; Yanyu Zhang, Yifei Zhang, and F.F. analyzed data; and Yanyu Zhang, H.L., and F.F. wrote the paper.

The authors declare no conflict of interest.

This article is a PNAS Direct Submission.

Published under the PNAS license.

[1]Yanyu Zhang and Yifei Zhang contributed equally to this work.

[2]To whom correspondence may be addressed. Email: ffang@pku.edu.cn or yanyuzhang@pku.edu.cn.

This article contains supporting information online at www.pnas.org/lookup/suppl/doi:10.1073/pnas.1904160116/-/DCSupplemental.

Published online August 5, 2019.

Downloaded at Palestinian Territory, occupied on December 7, 2021

www.manaraa.com

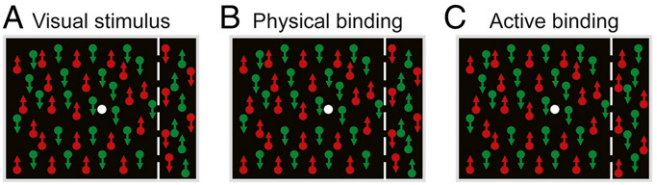

Fig. 1. Visual stimulus design. (*A*) The stimulus contains 2 sheets of dots: 1 sheet moving up and the other moving down. On both sheets, dots in the right peripheral area (right of the white dashed line, the effect part) and those in the rest area (left of the white dashed line, the induction part) are rendered with different colors (either red or green). Oppositely moving dots always have different colors. Thus, the induction and effect parts of the stimulus combine color and motion in opposite fashions. For the example stimulus here, on the upward-moving sheet, dots in the induction and effect parts are red and green, respectively. On the downward-moving sheet, dots in the induction and effect parts are green and red, respectively. Intriguingly, when observers fixate at the stimulus center, their perception of the binding of color and motion in the effect part is bistable, switching between the physical binding and the illusory binding. The illusory binding means that the color and motion of the dots in the effect part are erroneously perceived to be bound in the same fashion as those in the induction part. (*B*) The physical binding state. The color and motion of all of the dots are bound as their physical appearance. (*C*) The active (illusory) binding state. The illusory binding of color and motion causes observers to perceive upward-moving red dots and downward-moving green dots in the effect part. The illusory binding is actually an active binding process, in which the visual system treats the induction and effect parts as a unitary surface and relies on the information in the central induction part to make inferences about the properties of the peripheral effect part. The white dashed line is for illustration purposes only; it was not shown in the experiments.

specific frequency to individual subjects to examine how the stimulation might modulate their perceptual states. It is noteworthy that, because of volume conduction effects in EEG, even "local" α-oscillations are usually driven by large-scale brain networks. This is why we chose α-oscillations at some electrodes to index the dynamics of large-scale brain networks. We also performed interregional connectivity analyses with the EEG data. The connectivity results are presented in *SI Appendix*.

Results

Psychophysical Results. When subjects fixated at the center of the stimulus, the color and motion of the dots in the effect part were perceived as being bound either in the same fashion (active binding) as those in the induction part or in the opposite fashion (physical binding). On average, their perceptual states switched about every 13.640 s (SEM: 1.079). The mean durations of the active binding state and the physical binding state were 16.088 s (SEM: 1.707) and 11.192 s (SEM: 1.332). The former mean duration was significantly longer than the later one [$t(17) = 2.254$, $P = 0.038$].

EEG Results. We recorded subjects' continuous EEG signals when they performed the behavioral task and obtained the full power spectrum of the EEG signal epochs (100 to 1,100 ms after key press) using fast Fourier transform (FFT). Fig. 2*A* shows the group-averaged brain topographies of the power difference between the 2 perceptual states in θ- (4 to 7 Hz), α- (7 to 14 Hz), β- (14 to 30 Hz), and γ- (30 to 60 Hz) bands. For each band, the power was submitted to a repeated-measures ANOVA with perceptual state (physical binding and active binding) and electrode as within-subject factors. For the α-band, we found that the main effects of electrode [$F(60, 1{,}020) = 7.972$, $P = 0.004$] and perceptual state [$F(1, 17) = 12.069$, $P = 0.003$] were significant, while the interaction between perceptual state and electrode [$F(60, 1{,}020) = 1.033$, $P = 0.371$] was not significant. For the other 3 bands, the main effects of perceptual state [all $F(1, 17) < 1.711$, $P > 0.208$] and the interactions between perceptual state and electrode [all $F(60, 1{,}020) < 0.965$, $P > 0.363$] were not significant, and the main effects of electrode [all $F(60, 1{,}020) > 3.284$, $P < 0.033$] were significant. It is clear that there was significant α-power difference in the left posterior area (note that the perceptual state changes occurred in the right visual field in Fig. 2 *A* and *B*). In this area, we selected 10 electrodes with the largest differences as the region-of-interest (ROI), including P1, P3, P5, P7, Pz, PO3, PO7, POZ, O1, and Oz [all $t(17) > 2.597$, $P < 0.019$]. EEG signals from these electrodes were pooled together for further analysis.

In this ROI, the power was submitted to a repeated-measures ANOVA with perceptual state (physical binding and active binding) and frequency band (θ-, α-, β-, and γ-bands) as within-subject factors (Fig. 2 *C* and *D*). The interaction between perceptual state and frequency band was significant [$F(3, 51) = 3.893$, $P = 0.047$]. Both the main effects of frequency band [$F(3, 51) = 45.911$, $P < 0.001$] and perceptual state [$F(1, 17) = 8.095$, $P = 0.011$] were significant. Planned paired t tests showed that the α-power during the physical binding state was significantly larger than during the active binding state [$t(17) = 4.063$, $P = 0.001$], but no significant difference was found in the other frequency bands [all $t(17) < 1.718$, $P > 0.104$] (Fig. 2*D*). These findings suggest that α-activity might be important for feature binding, either physical binding or active binding or both.

To further evaluate the role of α-activity in feature binding and perceptual switch, we performed 2 correlation analyses. We first calculated the correlation coefficients between the percentage of time subjects perceived the active binding and the individual α-powers (IAPs) during the active and physical binding across individual subjects. The correlations were significant and negative (active binding: $r = -0.554$, $P = 0.008$, 1-tailed; physical binding: $r = -0.472$, $P = 0.024$, 1-tailed) (Fig. 3*A*). The larger the IAP, the shorter the active binding state. Second, we calculated the correlation coefficient between the individual α-frequency (IAF) and the perceptual switch rate across individual subjects and found that there was a significant positive correlation ($r = 0.549$, $P = 0.009$, 1-tailed) (Fig. 3*B*), suggesting that the individual α-peak frequency could predict the perceptual switch rate.

The EEG data analysis performed above was based on the 1,000-ms EEG epochs immediately following key press. We also tried to segment the continuous EEG signals during each perceptual state into epochs of 1,000 ms and then perform similar analyses. For the power in the ROI (i.e., the left posterior area), we found a significant interaction between perceptual state and frequency band [$F(3, 51) = 4.408$, $P = 0.021$]. Both the main effect of frequency [$F(3, 51) = 38.423$, $P < 0.001$] and the main effect of perceptual state [$F(1, 17) = 8.213$, $P = 0.011$] were significant. Planned paired t tests showed a significant power difference between 2 perceptual states in the α-band [$t(17) = 3.152$, $P = 0.006$], but not in the other bands [all $t(17) < 1.642$, $P > 0.119$]. We also found significant negative correlations between the percentage of time subjects perceived the active binding and the IAPs during the active and physical binding across individuals (active binding: $r = -0.440$, $P = 0.034$, 1-tailed; physical binding: $r = -0.498$, $P = 0.018$, 1-tailed) and a significant positive correlation between the IAF and the perceptual switch rate ($r = 0.507$, $P = 0.016$, 1-tailed) across subjects. Taken together, these 2 segmentation methods provide consistent evidence for the critical role of α-activity in feature binding and perceptual switch.

tACS Results. Since the EEG results can only provide correlational evidence of α-activity in feature binding, in the tACS experiments we examined whether subjects' perception (i.e., durations of perceptual states and perceptual switch rate) could be modulated by tACS. In tACS Exp. 1, we delivered continuous tACS over the left posterior area (PO3) at each subject's IAF to modulate α-activity. Meanwhile, subjects viewed the stimulus and reported their perceptual states by pressing 1 of 2 keys. We

Downloaded at Palestinian Territory, occupied on December 7, 2021
www.manaraa.com

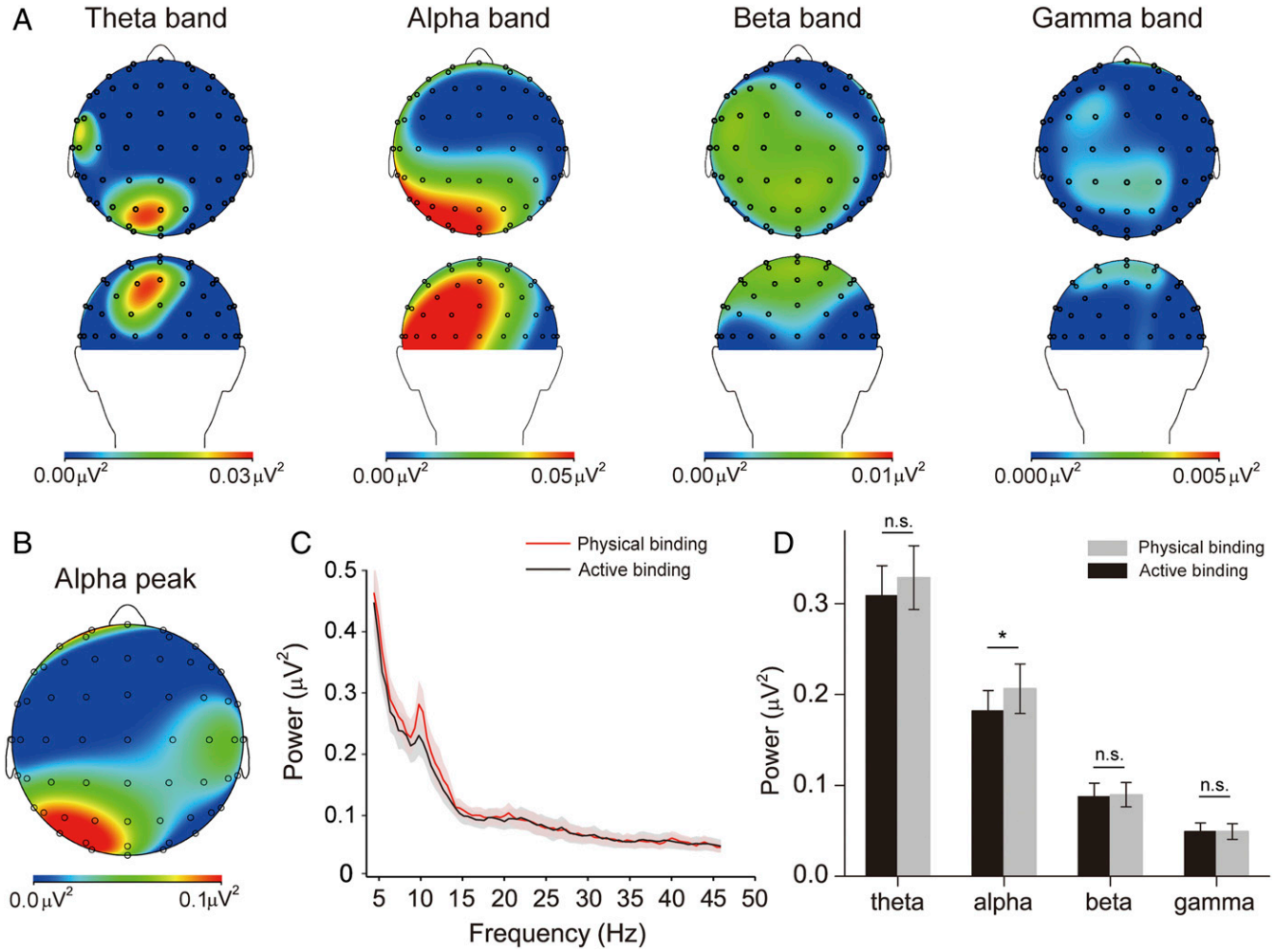

Fig. 2. EEG results. (*A*) Group-averaged brain topographies of power differences in different bands from top and back views. From left to right are topographies in the θ- (4 to 7 Hz), α- (7 to 14 Hz), β- (14 to 30 Hz), and γ- (30 to 60 Hz) bands. (*B*) Group-averaged brain topography of the α-peak power difference. (*C*) Group-averaged FFT power spectra for the physical binding state (light gray line) and the active binding state (dark gray line). The shaded areas represent 1 SEM calculated across subjects. (*D*) Group-averaged powers in the θ-, α-, β-, and γ-bands for the 2 binding states. Error bars represent 1 SEM calculated across subjects; n.s., not significant; $*P < 0.05$.

found that the continuous tACS decreased the proportion of the active binding time (mean ± SEM: 0.46 ± 0.06) relative to the sham stimulation (mean ± SEM: 0.65 ± 0.05). The difference between the 2 stimulation conditions was significant [$t(12) = 3.028$, $P = 0.011$] (Fig. 4*A*). Furthermore, in a control experiment (tACS Exp. 3), we examined whether the tACS effect was specific to the stimulation site. We applied continuous tACS over the right posterior area (PO4) and found that there was no significant

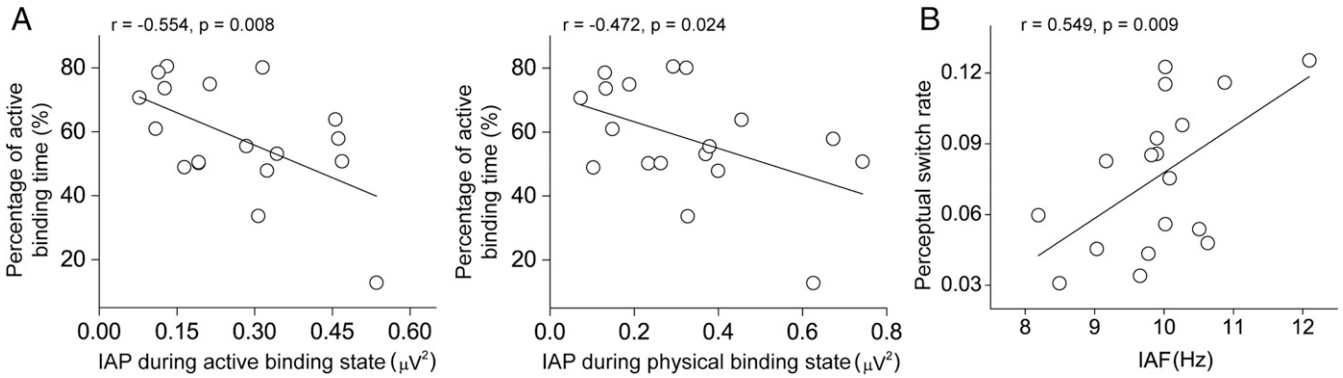

Fig. 3. Results of correlation analyses. (*A*) Correlations between the percentage of time subjects perceived the active binding and the IAPs during the active and physical binding across individual subjects. (*B*) Correlation between the IAF and the perceptual switch rate across individual subjects.

Downloaded at Palestinian Territory, occupied on December 7, 2021
www.manaraa.com

difference in the proportion of the active binding time between the sham stimulation condition (mean ± SEM: 0.46 ± 0.05) and the tACS condition (mean ± SEM: 0.48 ± 0.05) [$t(11) = 1.244$, $P = 0.240$].

In tACS Exp. 2, subjects received continuous tACS stimulation at 1 of 3 possible frequencies, including IAF, IAF − 2 Hz, and IAF + 2 Hz. We aimed to test whether driving IAF toward slower vs. faster oscillations would result in slower vs. faster perceptual switch, respectively. A 1-way repeated-measures ANOVA on perceptual switch rate showed that the main effect of tACS frequency was significant [$F(2, 24) = 4.351$, $P = 0.024$]. Post hoc paired t tests showed that the perceptual switch rate was significantly faster during tACS at IAF + 2 Hz (mean ± SEM: 0.103 ± 0.013) than during tACS at IAF − 2 Hz (mean ± SE: 0.075 ± 0.012) [$t(12) = 2.996$, $P = 0.011$] (Fig. 4*B*). The observed faster perceptual switch could be due to the shortening of perceptual epochs of the physical binding, the active binding, or both kinds of binding. Fig. 4*C* shows the average durations of perceptual epochs of the physical and active binding at the 3 tACS frequencies. One-way repeated-measures ANOVAs showed that the main effect of tACS frequency was significant for the active binding [$F(2, 24) = 3.935$, $P = 0.033$], but not for the physical binding [$F(2, 24) = 1.813$, $P = 0.201$], indicating that tACS mainly acted on the active binding process.

Discussion

Several major findings emerged in this study. First, IAP was negatively correlated with the time proportion of the active binding state. Second, subjects' perceptual switch rate was positively correlated with their IAF. Third, with the entrainment of α-oscillations by tACS, selectively changing α-oscillations could shape subjects' perceptual states of the color-motion binding. On the one hand, applying tACS at IAF could effectively decrease the time proportion of the active binding state. On the other hand, delivering tACS at different temporal frequencies in the α-band could change subjects' perceptual switch rates; tACS at a higher frequency led to a faster perceptual switch through shortening perceptual epochs of the active binding. α-Oscillations are the dominant oscillations in the human brain and are negatively correlated with cortical excitability and task performance. They are traditionally believed to represent idling processes in the brain and were recently viewed as a general inhibition mechanism for cognitive processing (26). Our findings provide strong evidence of the causal role of α-oscillations in feature binding, especially in active feature binding, which significantly advances our understanding of the functions of α-oscillations in human cognition.

In recent years, a growing body of research has suggested that α-activity is closely associated with conscious visual perception (27–29). α-Oscillations have been demonstrated to be able to dictate the resolution of conscious visual updating (24), to determine whether a visual stimulus could be perceived or not (30), to predict the stability of subjects' bistable perception (31), and to determine the perceived motion-direction changes when subjects were facing continuously moving objects (32). Here, we used a bistable color-motion binding stimulus and found that α-oscillations could trigger the switches between the two perceptual states and determine the dominant perceptual state, adding further evidence that α-band oscillations play a key role in visual perception and visual consciousness.

The decrease in the time proportion of the active binding state by applying tACS at IAF suggests that tACS might enhance IAP effectively, which is in line with previous studies (22, 33, 34). For example, Zaehle et al. (34) found that delivering tACS at subject's IAF could enhance α-power in human EEG. Additionally, the α-power increase induced by tACS could last for at least half an hour (33). Our finding that tACS at IAF ± 2 Hz modified subjects' perceptual switch rates indicates that tACS might interfere with the peak frequency of the α-band, which is also consistent with previous studies (23–25). Combining magnetoencephalography and tACS, Minami and Amano (25) demonstrated that the peak α-frequency was changed according to the target frequency for parieto-occipital tACS at IAF ± 1 Hz. Cecere et al. (23) also suggested a similar effective manipulation of the EEG peak α-frequency using tACS at IAF ± 2 Hz.

There has been a long, intense debate about the role of neural oscillations in the binding problem (12, 35–37). Some electrophysiological studies found that synchronized neuronal firing in the γ-band (~40 Hz) in monkey (14), cat (13), and human brains (15, 37, 38) was responsible for feature binding. However, this view has been challenged by some research groups (39, 40). Here, we found that α-band activities causally affected feature binding (active feature binding more profoundly). Some kinds of feature binding (e.g., the active binding here) require interactions among various brain areas (8, 9, 41). γ-Oscillations are typically restricted to monosynaptic connections and intraareal interactions (42), whereas α-oscillations are associated with long-range integrations and could provide a dynamic link among distributed visual areas (43, 44). Therefore, α-band activities might be necessary for feature binding requiring large-scale brain networks. Furthermore, γ-band synchronization modulates input gain and mediates feedforward connections (45, 46), whereas reentrant feedback influences are mediated by α-band activities (11, 19, 42). Accumulating evidence suggests that feature binding requires reentrant processing (7, 9), which further underscores the importance of α-oscillations in feature binding.

We observed that the α-power decreased during the active feature binding. In our recent fMRI study (9), using the same visual stimulus, we found that the active feature binding required

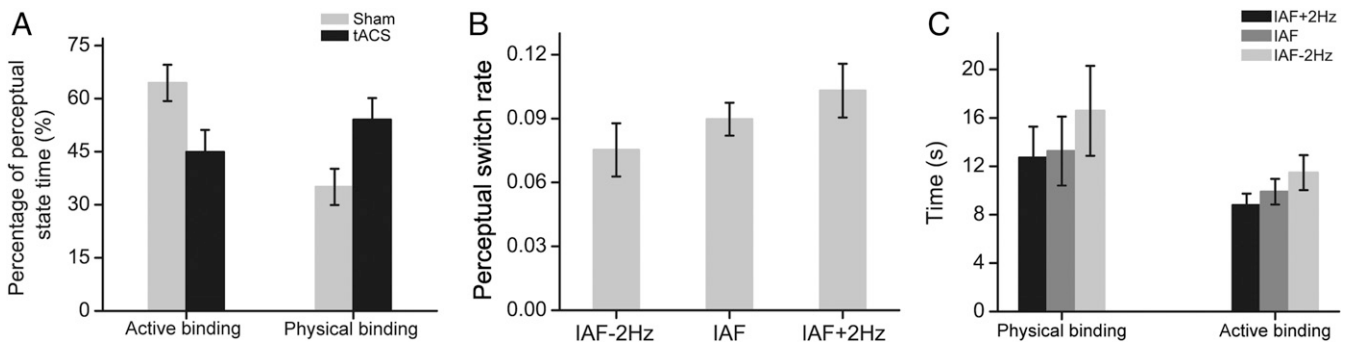

Fig. 4. Results of tACS experiments. (*A*) Percentages of perceptual state time for the physical and active binding in the sham stimulation condition and the tACS condition. (*B*) Perceptual switch rates under tACS at IAF, IAF − 2 Hz, and IAF + 2 Hz. (*C*) Averaged durations of perceptual epochs for the physical and active binding at the 3 tACS frequencies. Error bars represent 1 SEM calculated across subjects.

Downloaded at Palestinian Territory, occupied on December 7, 2021
www.manaraa.com

increased feedback connections from V4 and V5 to V2 and decreased feedforward connections from V2 to V4 and V5, whereas the physical binding relied on increased feedforward connections (also see ref. 47). In other words, when subjects switched to the active binding state, the representation of feedback connections was recruited and became more activated. Previous works found that α-band activities were essential in feedback processing (11) and were weaker when there were top-down or feedback influences (48, 49). Consistent with these findings, we found that the lower α-power accompanied the active binding, relative to the physical binding. This finding is also in line with Jensen et al.'s hypothesis (50) that α-band activity could control information flow dynamically. They argue that α-band activity reflects how many active representations could be processed simultaneously. If α-power increases or decreases, it means that fewer or more representations could be processed in one α-cycle. Notably, decreased α-activity is usually associated with a concurrent increase in interareal α-band phase synchrony (51, 52), which might be essential for the active binding.

We also found that α-oscillations could determine the perceptual switch rate between the 2 states, through affecting the active binding process specifically. Even though the perceptual switch rate was much lower than the individual α-frequency, there was a strong correlation between the individual α-frequency and the perceptual switch rate, indicating that α-band oscillations might serve as a basic temporal unit for feature binding. Temporal structure is one of the most important dimensions in visual information processing and timing is believed to be a fundamental function of α-band oscillations (53). With magnetoencephalography, Wutz et al. (54) found that there was a strong correlation between individual α-frequency and the temporal resolution of perception. They also found that the cycle of α-oscillations was the fundamental unit of temporal integration in visual perception. Minami and Amano (25) found that tACS could elongate or shorten the temporal window of motion-induced spatial conflict (i.e., an illusion involving motion and shape integration). α-Oscillations were also found to be an underlying mechanism of multisensory integration (23, 55). For example, Cecere et al. (23) showed that delivering tACS in the α-band over occipital regions could causally modulate the temporal window of visual–auditory integration. These findings provide converging evidence that α-band oscillations, serving as a temporal unit, could determine the integration of features, even from different sensory modalities.

It might be argued that our findings with α-oscillations can be simply explained by different attention levels during the 2 bindings. We have several reasons against this explanation. First, in the tACS experiments, we found that, when delivering tACS at different temporal frequencies in the α-band, subjects' perceptual switch rates changed correspondingly. To our best knowledge, no evidence has been found to show that attention is associated with α-frequency. Second, previous work found that attention could enhance γ-oscillations and synchrony in both humans and monkeys (56–58). However, we failed to find any significant difference in γ-oscillations and synchrony between the 2 bindings (Fig. 2*D* and *SI Appendix*, Figs. S1 and S2). Third, in our previous work (9), we did a whole-brain scan when subjects viewed the 2 bindings. A group analysis did not find any brain area (V1–V5 and posterior parietal cortex) showing differential responses to the 2 bindings. The dynamic causal modeling analysis also failed to find any significant difference in modulatory connectivity from the posterior parietal cortex (a key brain area in human attention network) to V2, V4, and V5 between the 2 bindings.

In conclusion, our findings here provide insights into not only the neural mechanisms of feature binding but also the functions of brain oscillations. We demonstrate that α-oscillations could determine the way of color-motion binding and that tACS is an effective approach to shaping feature binding. Our findings suggest that α-activity is an important neural substrate for feature binding, especially for active feature binding.

Materials and Methods

Subjects. Eighteen subjects (10 female, 19 to 27 y old) participated in the EEG experiment. Of the 18 subjects, 13 (6 female, 19 to 25 y old) also participated in tACS Exps. 1 and 2. Twelve subjects (9 female, 19 to 25 y old) participated in tACS Exp. 3 (3 new subjects and 9 of the subjects who had already taken part in tACS Exps. 1 and 2). In total, we recruited 21 subjects in this study. All subjects were naïve to the purpose of the study. They were right-handed, reported normal or corrected-to-normal vision, and had no known neurological or visual disorders. They each gave written informed consent before participating. Our experimental procedures were approved by the Human Subject Review Committee of Peking University.

Apparatus. Visual stimuli were displayed on Sony Trinitron monitors (model: MultiScan G520; resolution: 1,024 × 768; refresh rate: 100 Hz). Before the experiments, the monitors were calibrated with a MINOLTA CS-100A Chroma Meter. The viewing distance was 60 cm. During the experiments, we used a head and chin rest to stabilize subjects' head position.

Stimuli. Two stimuli were used in this study (Fig. 1). Each of them contained 2 sheets of random dots, 1 sheet moving up and the other moving down [sheet size: 29° × 26.5°; dot diameter: 0.11°; dot speed: 3°/s; dot luminance: 15 cd/m^2; dot density: 5/(°)^2]. Both stimuli were able to induce color-motion misbinding in the right peripheral area. On both sheets of these 2 stimuli, dots in the right peripheral area (6° × 26.5°, the effect part) and those in the rest area (23° × 26.5°, the induction part) were rendered with different colors, either red [CIE (1,931): $x = 0.614$, $y = 0.344$] or green [CIE (1,931): $x = 0.289$, $y = 0.593$]. For 1 stimulus, on the upward-moving sheet, dots in the effect and induction parts were red and green, respectively. On the downward-moving sheet, dots in the effect and induction parts were green and red, respectively. For the other stimulus, on the upward-moving sheet, dots in the effect and induction parts were green and red, respectively. On the downward-moving sheet, dots in the effect and induction parts were red and green, respectively. Subjects knew how the stimuli were designed and knew that the dot motion directions in the induction and effect parts were opposite.

EEG Experiment. The EEG experiment consisted of 16 blocks, 8 blocks for each of the 2 stimuli. At the beginning of a block, a white dot was presented at the center of the screen and subjects were instructed to fixate on the dot throughout the block. Six seconds later, 1 of the 2 visual stimuli was presented for 180 s. Subjects were asked to press 1 of 2 keys to indicate their perceptual state, either the physical binding state or the active binding state. Meanwhile, continuous EEG was recorded from 64 sintered Ag/AgCl electrodes positioned according to the extended international 10 to 20 EEG system. Vertical electrooculogram was recorded from an electrode placed above the right eye. Horizontal EOG was recorded from an electrode placed at the outer canthus of the left eye. Electrode impedance was kept below 5 kΩ. EEG was amplified with a gain of 500 K, band pass-filtered at 0.05 to 100 Hz, and digitized at a sampling rate of 1,000 Hz. The signals from these electrodes were referenced online to the tip of the nose and were rereferenced offline to the average of the 2 mastoids.

Offline EEG data analysis was performed using Brain Vision Analyzer (Brain Products). We took 2 approaches to segment the continuous EEG signals into epochs of 1,000 ms. In the first approach, the epochs were from 100 ms to 1,100 ms after subjects' key press. In the second approach, the EEG signals were segmented starting at 100 ms after a key press and ending at 1,000 ms before the immediate next key press. Epochs contaminated by eye blinks, eye movements, or muscle potentials and exceeding ±100 μV at any electrode were excluded from analysis. To make sure that there was only 1 perceptual state during an epoch, we excluded those epochs during which subjects made more than 1 response. The full power spectrums of the remaining epochs were obtained through a FFT and were then pooled together according to subjects' perceptual state (physical binding vs. active binding). For each subject, IAF was defined as the frequency within the 8- to 14-Hz range that exhibited the largest power difference between the physical binding and the active binding, which was almost identical to the peak frequencies within the 8- to 14-Hz range for both kinds of binding. IAP was the power value at the IAF.

tACS Experiments. tACS was delivered by a battery-powered DC stimulator (Neuroconn) through a pair of rubber electrodes enclosed in saline-soaked sponges and fixed on the head by 4 elastic bands. The reference electrode and the stimulation electrode were placed over the vertex and the left

Downloaded at Palestinian Territory, occupied on December 7, 2021

www.manaraa.com

posterior area (Cz and PO3 in the international 10 to 20 EEG system), respectively. The size of the electrodes was 35 cm^2. We used a sinusoidal current and set DC offset at 0. The impedance was kept below 10 kΩ. The intensity of the current was initially set at 2 mA. We asked subjects to report any perception of tACS-induced phosphenes throughout the experiments. For participants reporting perception of phosphenes, the intensity was lowered in 0.1-mA steps until no phosphene was perceived. In our study, the mean stimulation intensity was 1.43 mA.

In tACS Exp. 1, subjects underwent 2 experimental sessions (the IAF session and the sham session) spaced 40-min apart from each other to avoid any carryover effect from the preceding session (33). In each session, they performed 6 blocks of the behavioral task (same as that in the EEG experiment) while receiving continuous tACS at PO3 at IAF Hz or receiving sham stimulation. The sham session was identical to the IAF session except that we kept the stimulator off during the "stimulation" period.

tACS Exp. 2 was very similar to tACS Exp. 1 except that it had 4 experimental sessions: The IAF session, the IAF − 2 session, the IAF + 2 session, and the sham session. In the IAF ± 2 sessions, subjects received continuous tACS at IAF ± 2 Hz, respectively. tACS Exp. 3 served as a control experiment for tACS Exp. 1. These 2 experiments were identical except that tACS was delivered over the right posterior area (PO4) in tACS Exp. 3. In all of the tACS experiments, the session order was randomized across subjects.

ACKNOWLEDGMENTS. This work was supported by Ministry of Science and Technology Grant 2015CB351800; National Science Foundation of China Grants 31421003, NSFC 61527804, and NSFC 31671168; and Beijing Municipal Science and Technology Commission Grant Z181100001518002.

1. M. Livingstone, D. Hubel, Segregation of form, color, movement, and depth: Anatomy, physiology, and perception. *Science* **240**, 740–749 (1988).
2. A. Treisman, The binding problem. *Curr. Opin. Neurobiol.* **6**, 171–178 (1996).
3. A. O. Holcombe, P. Cavanagh, Early binding of feature pairs for visual perception. *Nat. Neurosci.* **4**, 127–128 (2001).
4. K. Seymour, C. W. Clifford, N. K. Logothetis, A. Bartels, The coding of color, motion, and their conjunction in the human visual cortex. *Curr. Biol.* **19**, 177–183 (2009).
5. R. Desimone, J. Duncan, Neural mechanisms of selective visual attention. *Annu. Rev. Neurosci.* **18**, 193–222 (1995).
6. W. Braet, G. W. Humphreys, The role of reentrant processes in feature binding: Evidence from neuropsychology and TMS on late onset illusory conjunctions. *Vis. Cogn.* **17**, 25–47 (2009).
7. S. Bouvier, A. Treisman, Visual feature binding requires reentry. *Psychol. Sci.* **21**, 200–204 (2010).
8. M. Koivisto, J. Silvanto, Visual feature binding: The critical time windows of V1/V2 and parietal activity. *Neuroimage* **59**, 1608–1614 (2012).
9. X. Zhang, J. Qiu, Y. Zhang, S. Han, F. Fang, Misbinding of color and motion in human visual cortex. *Curr. Biol.* **24**, 1354–1360 (2014).
10. M. Usher, N. Donnelly, Visual synchrony affects binding and segmentation in perception. *Nature* **394**, 179–182 (1998).
11. P. Fries, Rhythms for cognition: Communication through coherence. *Neuron* **88**, 220–235 (2015).
12. W. Singer, C. M. Gray, Visual feature integration and the temporal correlation hypothesis. *Annu. Rev. Neurosci.* **18**, 555–586 (1995).
13. C. M. Gray, W. Singer, Stimulus-specific neuronal oscillations in orientation columns of cat visual cortex. *Proc. Natl. Acad. Sci. U.S.A.* **86**, 1698–1702 (1989).
14. M. A. Elliott, H. J. Müller, Synchronous information presented in 40-Hz flicker enhances visual feature binding. *Psychol. Sci.* **9**, 277–283 (1998).
15. C. Tallon-Baudry, O. Bertrand, Oscillatory gamma activity in humans and its role in object representation. *Trends Cogn. Sci.* **3**, 151–162 (1999).
16. A. Arieli, D. Shoham, R. Hildesheim, A. Grinvald, Coherent spatiotemporal patterns of ongoing activity revealed by real-time optical imaging coupled with single-unit recording in the cat visual cortex. *J. Neurophysiol.* **73**, 2072–2093 (1995).
17. J. Csicsvari, B. Jamieson, K. D. Wise, G. Buzsáki, Mechanisms of gamma oscillations in the hippocampus of the behaving rat. *Neuron* **37**, 311–322 (2003).
18. S. Palva, J. M. Palva, Discovering oscillatory interaction networks with M/EEG: Challenges and breakthroughs. *Trends Cogn. Sci.* **16**, 219–230 (2012).
19. G. Michalareas *et al*., Alpha-beta and gamma rhythms subserve feedback and feedforward influences among human visual cortical areas. *Neuron* **89**, 384–397 (2016).
20. D. A. Wu, R. Kanai, S. Shimojo, Vision: Steady-state misbinding of colour and motion. *Nature* **429**, 262 (2004).
21. Y. Zhang, X. Zhang, Y. Wang, F. Fang, Misbinding of color and motion in human early visual cortex: Evidence from event-related potentials. *Vision Res.* **122**, 51–59 (2016).
22. R. F. Helfrich *et al*., Entrainment of brain oscillations by transcranial alternating current stimulation. *Curr. Biol.* **24**, 333–339 (2014).
23. R. Cecere, G. Rees, V. Romei, Individual differences in alpha frequency drive cross-modal illusory perception. *Curr. Biol.* **25**, 231–235 (2015).
24. J. Samaha, B. R. Postle, The speed of alpha-band oscillations predicts the temporal resolution of visual perception. *Curr. Biol.* **25**, 2985–2990 (2015).
25. S. Minami, K. Amano, Illusory jitter perceived at the frequency of alpha oscillations. *Curr. Biol.* **27**, 2344–2351.e4 (2017).
26. W. Klimesch, P. Sauseng, S. Hanslmayr, EEG alpha oscillations: The inhibition-timing hypothesis. *Brain Res. Brain Res. Rev.* **53**, 63–88 (2007).
27. O. Jensen, M. Bonnefond, R. VanRullen, An oscillatory mechanism for prioritizing salient unattended stimuli. *Trends Cogn. Sci.* **16**, 200–206 (2012).
28. E. Spaak, F. P. de Lange, O. Jensen, Local entrainment of α oscillations by visual stimuli causes cyclic modulation of perception. *J. Neurosci.* **34**, 3536–3544 (2014).
29. J. Jia, L. Liu, F. Fang, H. Luo, Sequential sampling of visual objects during sustained attention. *PLoS Biol.* **15**, e2001903 (2017).
30. S. Hanslmayr, J. Gross, W. Klimesch, K. L. Shapiro, The role of α oscillations in temporal attention. *Brain Res. Rev.* **67**, 331–343 (2011).
31. G. Piantoni, N. Romeijn, G. Gomez-Herrero, Y. D. Van Der Werf, E. J. W. Van Someren, Alpha power predicts persistence of bistable perception. *Sci. Rep.* **7**, 5208 (2017).
32. R. VanRullen, L. Reddy, C. Koch, The continuous wagon wheel illusion is associated with changes in electroencephalogram power at approximately 13 Hz. *J. Neurosci.* **26**, 502–507 (2006).
33. T. Neuling, S. Rach, C. S. Herrmann, Orchestrating neuronal networks: Sustained after-effects of transcranial alternating current stimulation depend upon brain states. *Front. Hum. Neurosci.* **7**, 161 (2013).
34. T. Zaehle, S. Rach, C. S. Herrmann, Transcranial alternating current stimulation enhances individual alpha activity in human EEG. *PLoS One* **5**, e13766 (2010).
35. W. Singer, Neuronal synchrony: A versatile code for the definition of relations? *Neuron* **24**, 49–65, 111–125 (1999).
36. P. R. Roelfsema, V. A. F. Lamme, H. Spekreijse, Synchrony and covariation of firing rates in the primary visual cortex during contour grouping. *Nat. Neurosci.* **7**, 982–991 (2004).
37. M. Rose, T. Sommer, C. Büchel, Integration of local features to a global percept by neural coupling. *Cereb. Cortex* **16**, 1522–1528 (2006).
38. C. Tallon-Baudry, O. Bertrand, C. Delpuech, J. Pernier, Stimulus specificity of phase-locked and non-phase-locked 40 Hz visual responses in human. *J. Neurosci.* **16**, 4240–4249 (1996).
39. A. Thiele, G. Stoner, Neuronal synchrony does not correlate with motion coherence in cortical area MT. *Nature* **421**, 366–370 (2003).
40. B. J. Palanca, G. C. DeAngelis, Does neuronal synchrony underlie visual feature grouping? *Neuron* **46**, 333–346 (2005).
41. G. Tononi, O. Sporns, G. M. Edelman, Reentry and the problem of integrating multiple cortical areas: Simulation of dynamic integration in the visual system. *Cereb. Cortex* **2**, 310–335 (1992).
42. A. von Stein, C. Chiang, P. König, Top-down processing mediated by interareal synchronization. *Proc. Natl. Acad. Sci. U.S.A.* **97**, 14748–14753 (2000).
43. A. von Stein, J. Sarnthein, Different frequencies for different scales of cortical integration: From local gamma to long range alpha/theta synchronization. *Int. J. Psychophysiol.* **38**, 301–313 (2000).
44. J. van Driel, T. Knapen, D. M. van Es, M. X. Cohen, Interregional alpha-band synchrony supports temporal cross-modal integration. *Neuroimage* **101**, 404–415 (2014).
45. E. A. Buffalo, P. Fries, R. Landman, T. J. Buschman, R. Desimone, Laminar differences in gamma and alpha coherence in the ventral stream. *Proc. Natl. Acad. Sci. U.S.A.* **108**, 11262–11267 (2011).
46. A. M. Bastos *et al*., Visual areas exert feedforward and feedback influences through distinct frequency channels. *Neuron* **85**, 390–401 (2015).
47. S. Shipp, D. L. Adams, K. Moutoussis, S. Zeki, Feature binding in the feedback layers of area V2. *Cereb. Cortex* **19**, 2230–2239 (2009).
48. P. Fries, T. Womelsdorf, R. Oostenveld, R. Desimone, The effects of visual stimulation and selective visual attention on rhythmic neuronal synchronization in macaque area V4. *J. Neurosci.* **28**, 4823–4835 (2008).
49. F. van Ede, F. de Lange, O. Jensen, E. Maris, Orienting attention to an upcoming tactile event involves a spatially and temporally specific modulation of sensorimotor alpha- and beta-band oscillations. *J. Neurosci.* **31**, 2016–2024 (2011).
50. O. Jensen, B. Gips, T. O. Bergmann, M. Bonnefond, Temporal coding organized by coupled alpha and gamma oscillations prioritize visual processing. *Trends Neurosci.* **37**, 357–369 (2014).
51. R. Freunberger, R. Fellinger, P. Sauseng, W. Gruber, W. Klimesch, Dissociation between phase-locked and nonphase-locked alpha oscillations in a working memory task. *Hum. Brain Mapp.* **30**, 3417–3425 (2009).
52. J. M. Palva, S. Monto, S. Kulashekhar, S. Palva, Neuronal synchrony reveals working memory networks and predicts individual memory capacity. *Proc. Natl. Acad. Sci. U.S.A.* **107**, 7580–7585 (2010).
53. W. Klimesch, α-band oscillations, attention, and controlled access to stored information. *Trends Cogn. Sci.* **16**, 606–617 (2012).
54. A. Wutz, D. Melcher, J. Samaha, Frequency modulation of neural oscillations according to visual task demands. *Proc. Natl. Acad. Sci. U.S.A.* **115**, 1346–1351 (2018).
55. V. Romei, J. Gross, G. Thut, Sounds reset rhythms of visual cortex and corresponding human visual perception. *Curr. Biol.* **22**, 807–813 (2012).
56. H. Tiitinen *et al*., Selective attention enhances the auditory 40-Hz transient response in humans. *Nature* **364**, 59–60 (1993).
57. P. Fries, J. H. Reynolds, A. E. Rorie, R. Desimone, Modulation of oscillatory neuronal synchronization by selective visual attention. *Science* **291**, 1560–1563 (2001).
58. O. Jensen, J. Kaiser, J. P. Lachaux, Human gamma-frequency oscillations associated with attention and memory. *Trends Neurosci.* **30**, 317–324 (2007).

Downloaded at Palestinian Territory, occupied on December 7, 2021
www.manaraa.com